

## Zero-Valent Iron Nanoparticles (NZVI) Supported by Zeolite Clinoptilolite-Supported for Removal of Cu(II) Ions by Adsorption: A Optimization Study by Response Surface Methodology (RSM)

P. Gharbani<sup>a,b,\*</sup>

<sup>a</sup>Department of Chemistry, Ahar Branch, Islamic Azad University, Ahar, Iran

<sup>b</sup>Industrial Nanotechnology Research Center, Tabriz Branch, Islamic Azad University, Tabriz, Iran

(Received 18 July 2023, Accepted 21 September 2023)

In this study, nanoscale zero-valent iron supported onto Zeolite Clinoptilolite (NZVI/Zeolite) was synthesized from a facile method as an adsorbent for removing Cu(II) from aqueous solutions. Field Emission Scanning Electron Micrographs (FESEM) showed no aggregation, and dot mapping revealed the uniform dispersion of iron onto the surface of the zeolite. The surface area of synthesized NZVI/Zeolite was obtained at about  $132.14 \text{ m}^2 \text{ g}^{-1}$  by BET analysis. Also, the isotherm adsorption of Cu(II) onto NZVI/Zeolite was best fitted with the Temkin isotherm ( $R^2 = 0.894$ ) and maximum adsorption capacity ( $q_m$ ) of Cu(II) onto NZVI/Zeolite was  $61.72 \text{ mg g}^{-1}$ . The maximum removal of Cu(II) by NZVI/Zeolite was about 99.98% at  $\text{pH} = 8$ , the dosage of adsorbent =  $0.1 \text{ mg l}^{-1}$ , Cu(II) concentration =  $60 \text{ mg l}^{-1}$ , and time = 30 min. The reusability of nanocomposite after five consecutive cycles showed a 12.72% reduction in the removal of Cu(II). These results suggest that NZVI/Zeolite has excellent potential for the removal of Cu(II) from aqueous solutions.

**Keywords:** Zeolite Clinoptilolite, Zero-valent iron, Heavy metals, Isotherm, Copper

### INTRODUCTION

With the development of industrial activities and population growth, the release of heavy metals into the environment is increasing, which has become one of the environmental problems. Heavy metals are not metabolized in the body and can accumulate in the body and lead to various diseases. Heavy metals are released into the environment in various industrial processes such as smelting, purification, and extraction of metals through the emission of polluted gases and industrial effluents. These metals cannot be decomposed and leave toxic effects in the body of organisms [1]. Large amounts of heavy metals enter the environment naturally and through various methods such as rock erosion, dust particles, volcanic activity, rivers, and

underground water. But the main problem is the increase in the amount of these metals due to human activities such as oil pollution, increase in industrial effluents, *etc.* [2]. Different methods have been used to remove heavy metals from aqueous solutions, such as chemical precipitation, ion exchange, adsorption, and reverse osmosis [3]. The adsorption method is one of the most widely used methods due to its efficiency and easy application [4]. A lot of research has been done on carbon nanotubes, clay minerals, nano metal oxides (NMOs), activated carbon, and graphene oxides as efficient adsorbents in the removal of heavy metals [5,6]. One of the most widely used adsorbents is nano-scale zero-valent iron (NZVI) with high reactivity, which is an environmentally friendly material for removing various metal ions from aqueous solutions. It is used because of controllable particle size, high reactivity, and many reactive surface sites [7,8]. The extraordinary physical and chemical properties of NZVI make it an effective reagent, but some

\*Corresponding author. E-mail: [parvingharbani@yahoo.com](mailto:parvingharbani@yahoo.com)

environmental factors complicate its practical application. Small NZVI particles should be mobile, but they tend to agglomerate due to nanoscale magnetic and electrostatic attraction and high surface energy through van der Waals forces. In addition, in the preparation of NZVI, expensive reducing agents such as NaBH<sub>4</sub> are used, and this process is complicated and time-consuming with several steps of centrifugation, washing, and drying. In addition, the potential toxicity of NZVI can be a problem in large-scale applications [9]. Combining NZVI with clinoptilolite zeolite may help to solve these problems, because of its high ion exchange capacity and high internal and external surfaces [10]. Another important feature of clinoptilolite zeolite is its ability to be regenerated while maintaining its original properties. Zeolite belongs to the hydrated aluminosilicate family of alkali and alkaline earth metals that have a crystalline and tetrahedral structure (four oxygen atoms around one silicon atom). Their three important features are ion exchange, surface adsorption, and catalyst due to the structural properties of zeolites, which has caused them to be widely used in various branches of industry, especially in environmental processes [10]. Nanoscale Zero-Valent Iron (NZVI) supported on senegeles waste was used for removal of Pb(II) from the aqueous solution [7]. Zeolite-supported microscale zero-valent iron was applied to remove Cr<sup>6+</sup> and Cd<sup>2+</sup> from the aqueous solution [7]. Also, the removal of lead with zero-valent iron nanoparticles based on zeolite and Montmorillonite was studied [11]. As known, adsorption is greatly influenced by the characteristics of the adsorbent and solution, and it is very important to evaluate the effects of different factors in adsorption studies. Most conventional studies investigating adsorption characteristics are based on the results of a single-factor approach to time, in which a single factor is a variable while the remaining variables are fixed. This approach has the advantage of being able to examine the individual effects of each variable in detail. However, the actual adsorption response is not only affected by the individual effects of each variable but also by the interactions between multiple variables. Design of Experiment (DOE) is a systematic procedure to determine the relationships between factors affecting a process and its outputs through a limited number of experiments. Among the various DOE-based methods, the response surface methodology (RSM) is widely used because it is efficient in statistically interpreting the effect of each

variable, interaction and optimizing the responses [12,13]. In the current research, zero-valent iron nanoparticles were prepared based on Clinoptilolite zeolite, and after screening, the effect of independent variables such as pH, reaction time, adsorbent dose, and initial concentration of Cu(II) on Cu(II) adsorption by NZVI/Zeolite was investigated and optimized using RSM. Also, adsorption isotherms were determined under optimal conditions.

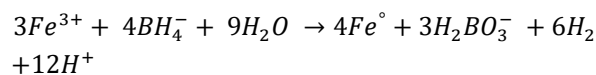
## MATERIALS AND METHODS

### Materials

Iron(III) chloride. 6H<sub>2</sub>O (FeCl<sub>3</sub>·6H<sub>2</sub>O), sodium tetrahydroborate (NaBH<sub>4</sub>), copper sulfate. 5H<sub>2</sub>O (CuSO<sub>4</sub>·5H<sub>2</sub>O), hydrochloric acid (HCl), sodium hydroxide (NaOH), and ethanol (C<sub>2</sub>H<sub>5</sub>OH) were obtained from Merck, Germany. Zeolite Clinoptilolite (((Na,K)<sub>6</sub>(Al<sub>6</sub>Si<sub>3</sub>O)<sub>72</sub>·nH<sub>2</sub>O)) was also obtained from Afrazand Semnan Company of Iran.

### Synthesis of Nano Zero-valent Iron/Zeolite

The nano zero-valent iron/zeolite was synthesized via a simple method. In brief, 1.62 g of FeCl<sub>3</sub>·6H<sub>2</sub>O, 1 g of Clinoptilolite zeolite, and 100 ml of deionized water were poured into a 500 ml three-necked flask and stirred for half an hour. The pH of the solution is controlled at 3 using NaOH (0.96 M). Then it was ultrasound for 45 min. To reduction of Fe(III), the mixed NaBH<sub>4</sub> (0.96 M) and NaOH (1:9) was added to the above solution drop by drop and stirred for 45 min. Spontaneously 10 ml of ethanol was added. The obtained solutions were changed to black and NZVI/Zeolite was formed. The reduction of Fe(III) occurred as follows:



Then it was filtered and washed three times with distillation water and ethanol. It was dried in a vacuum oven at 60 °C for 8 h [14].

### Adsorption Experimental

To perform the Cu(II) adsorption experiments onto NZVI/Zeolite, four independent variables of initial concentration (30, 60, 90, 120, 150 mg l<sup>-1</sup>), pH (2, 4, 6, 8, 10), dosage (0.05, 0.1, 0.15, 0.2, 0.25 mg l<sup>-1</sup>) and time (10, 20, 30,

40, 50 min) were selected (Table 1). 30 tests were suggested by DOE software. Firstly, solutions of Cu(II) with desired concentration and pH were prepared. Then, a specific amount of adsorbent was added, and a sample was taken from the

solution at a specific time. The solutions were filtered and the amount of Cu(II) was recorded using atomic absorption spectroscopy and was obtained from Eq. (1):

$$\%Removal = \frac{(C_0 - C_t)}{C_0} \times 100 \quad (1)$$

**Table 1.** Levels of the Parameters and 30 Designed Experiments

Parameter	Levels				
	-2 (- $\alpha$ )	-1	0	+1	+2 (+ $\alpha$ )
$x_1$ : [Cu <sup>2+</sup> ] <sub>0</sub> (mg l <sup>-1</sup> )	30	60	90	120	150
$x_2$ : [NZVI/Zeolite] <sub>0</sub> (g 50 ml <sup>-1</sup> )	0.05	0.1	0.15	0.2	0.25
$x_3$ : pH	2	4	6	8	10
$x_4$ : Time (min)	10	20	30	40	50

Run	Parameter values				Removal (%)
	$x_1$	$x_2$	$x_3$	$x_4$	Exp.
1	0.1	120	4	40	45.49
2	0.1	60	4	40	81.91
3	0.15	90	6	50	93.95
4	0.2	60	4	20	95.87
5	0.15	90	6	30	93.32
6	0.1	60	8	20	99.98
7	0.25	90	6	30	99.86
8	0.1	120	8	40	92.45
9	0.15	90	6	30	95.92
10	0.2	60	8	20	98.33
11	0.2	60	8	40	92.3
12	0.15	90	6	30	94.98
13	0.2	60	4	40	99.91
14	0.1	120	8	20	90.9
15	0.2	120	4	20	80.21
16	0.2	120	8	40	97.01
17	0.1	60	4	20	67.43
18	0.2	120	8	20	99.29
19	0.05	90	6	30	62.27
20	0.1	60	8	40	98.93
21	0.15	90	6	30	91.48
22	0.15	90	10	30	93.88
23	0.1	120	4	20	32.41
24	0.15	90	6	10	96.49
25	0.15	90	2	30	39.45
26	0.15	90	6	30	95.83
27	0.15	30	6	30	99.92
28	0.2	120	4	40	85.24
29	0.15	150	6	30	79.02
30	0.15	90	6	30	94.55

In this regard,  $C_0$  is the initial concentration ( $\text{mg l}^{-1}$ ) and  $C_t$  is the concentration of the Cu(II) at various times.

### Analysis

The prepared NZVI/Zeolite was characterized by Spectrum Two FTIR spectrophotometer (PerkinElmer) and the crystalline properties of it was analyzed using X-ray diffraction (XRD, X'Pert Pro, Analytical), from 10 to 80 using Cu Ka ( $1.54 \text{ \AA}$ ) as an X-ray source. The surface morphology was investigated by Field emission scanning electron microscopy (FE-SEM, SIGMA VP-500, Zeiss) equipped with EDS (energy dispersive X-ray spectroscopy) and dot Mapping of England Oxford Instruments. Also, the nanocomposite was analyzed by Transmission Electron Microscope (TEM Zeiss-EM10C-100 KV, Germany). BELSORP mini II (MicrotracBEL Corp., Osaka, Japan) was used to measure surface area. The concentration of Cu(II) was recorded using atomic absorption spectroscopy (VARIAN AA240).

## RESULTS AND DISCUSSION

### Characterization

FTIR analysis of NZVI/Zeolite was shown in Fig. 1a. The appeared spectra at wavelengths less than  $900 \text{ cm}^{-1}$  are related to the Al-O and Si-O and the peak in the region of  $3425 \text{ cm}^{-1}$  is related to the presence of O-H bond tensile vibrations in the molecules of water [15]. The observed band at  $1633 \text{ cm}^{-1}$  is related to the C=O bond, which occurred as a result of the cellular uptake of  $\text{CO}_2$ . The absorption band observed at  $1424 \text{ cm}^{-1}$  is related to the Fe-O structure in NZVI that confirms the NZVI nanoparticles were successfully coating on the surface of zeolite [16]. The broadband in the region of  $1062 \text{ cm}^{-1}$  is the result of Al-O-Si vibration [17]. X-ray diffraction pattern of NZVI/Zeolite shows (Fig. 1b) clinoptilolite zeolite ( $\text{Na,K,Ca})_2\text{-}_3\text{Al}_3(\text{Al,Si})_2\text{Si}_{13}\text{O}_{36}\cdot 12\text{H}_2\text{O}$ ) unit cell parameters are as follows:  $a = 17.62 \text{ \AA}$ ,  $b = 17.95 \text{ \AA}$ ,  $c = 7.39 \text{ \AA}$  and  $\beta = 116^\circ$  [18]. The XRD patterns of NZVI/Zeolite showed the diffraction peaks at  $2\theta =$  of  $35.5^\circ$ ,  $62.5^\circ$  for  $\text{Fe}_2\text{O}_3$ ,  $2\theta = 30^\circ$  for  $\text{FeOOH}$ , and  $2\theta = 44.1^\circ$  for  $\text{Fe}^0$ . The small peak of  $\text{Fe}^0$  may be due to the strong oxidation of  $\text{Fe}^0$  on the surface of zeolite [19].

FESEM images of zero-valent iron nanoparticles based

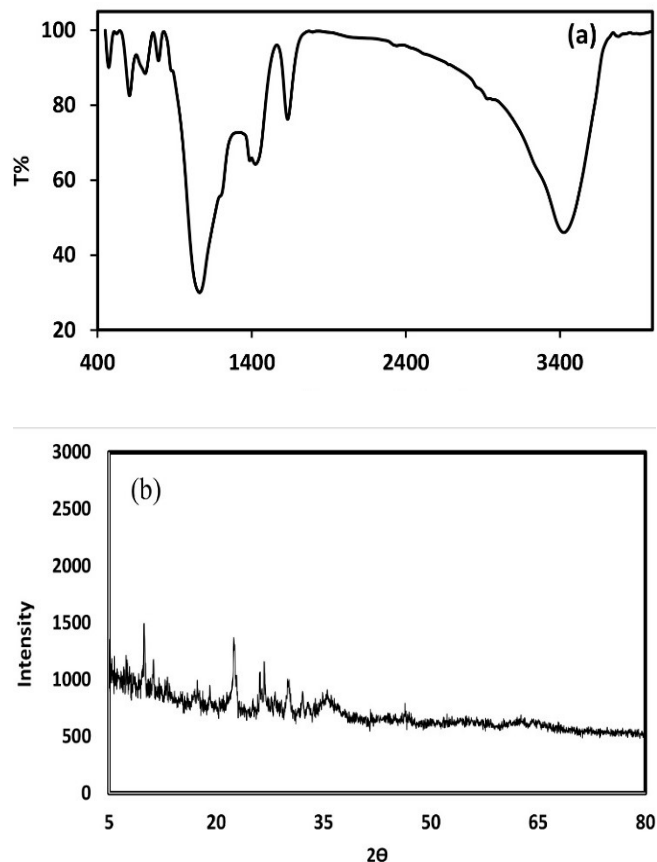


Fig. 1. a) FTIR and b) XRD of NZVI/Zeolite.

on zeolite with different magnifications are shown in Fig. 2. According to Fig. 2, the  $\text{Fe}_3\text{O}_4$  nanoparticles are spherical and are uniformly distributed on the surface of the zeolite. As seen, the average particle size is about 35 nm. EDX results of zero-valent iron nanoparticles based on zeolite (Fig. 1s) show that the synthesized composition contains 27.54% of Si, 25.57% of Fe, 25.54% of oxygen, 8.91% of Na, and 8.38% of Al, 2.56% of K and 1.79% of Ca.

According to the FESEM and dot mapping of NZVI/Zeolite, the distribution of iron nanoparticles on the surface of zeolite is completely uniform, which confirms the uniform distribution of iron nanoparticles onto zeolite (Fig. 2s). Distribution of NZVI (10-100 nm) on the surface of MCM zeolite revealed that NZVI has a small  $\text{Fe}^0$  core and iron oxide shell that confirmed the presence of a Fe-shell layer on the nanocomposite [20]. Also, the prepared

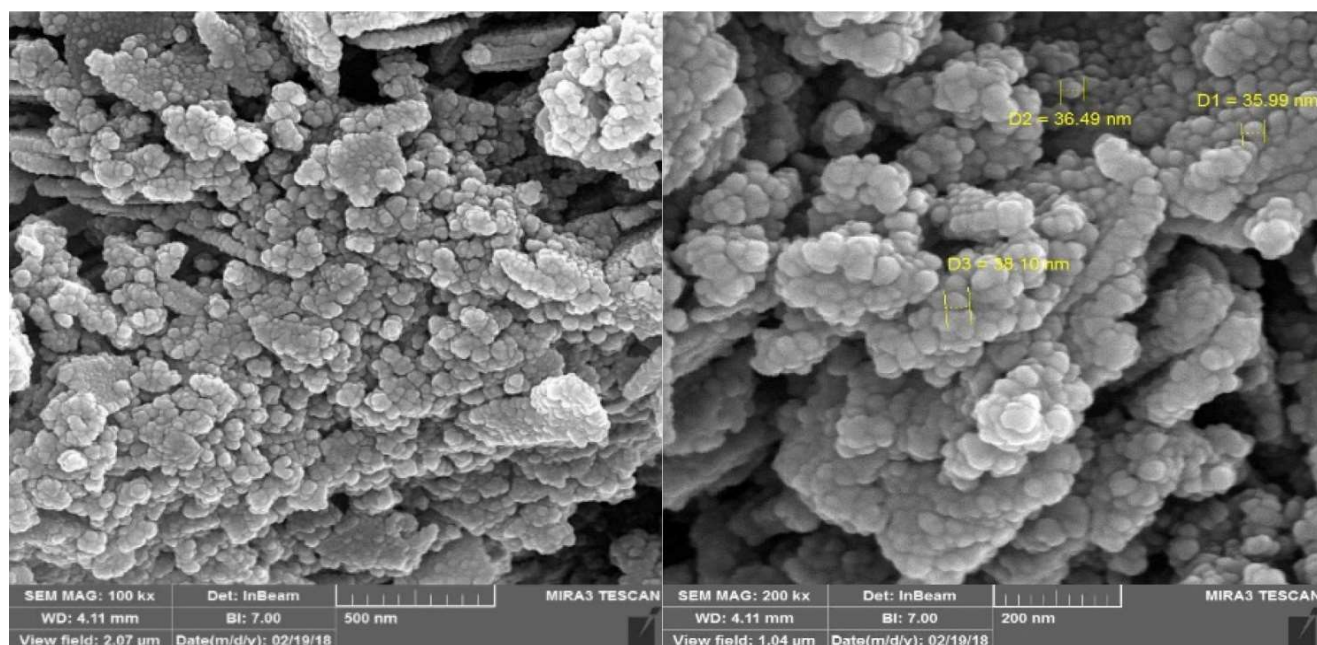


Fig. 2. FESEM of NZVI/Zelite.

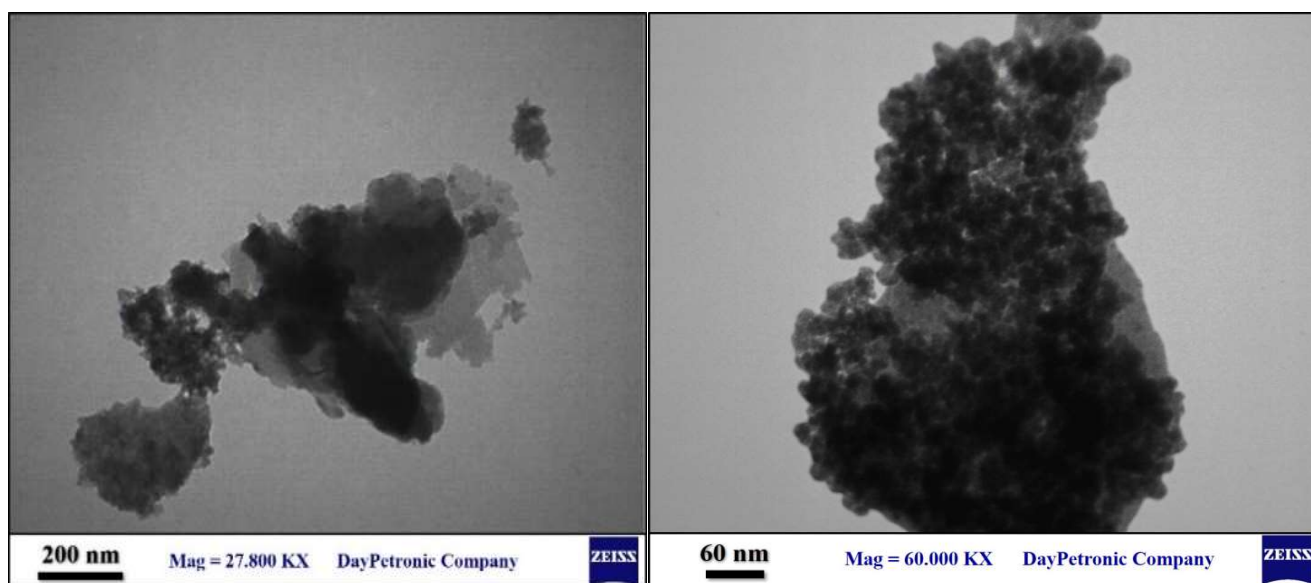


Fig. 3. TEM of NZVI/Zelite a) 200 nm, b) 60 nm.

NZVI/Zelite by Arancibia-Miranda showed the size distribution of particles with a mean diameter of 69.8 nm [11].

The results of BET analysis showed that the surface area of synthesized NZVI/Zelite is equal to 132.14 m<sup>2</sup> g<sup>-1</sup>, the pore diameter is 7.33 nm, and their internal volume is

0.242 cm<sup>3</sup> g<sup>-1</sup> (Table 1s). These results confirmed the high potential of the synthesized NZVI/Zelite as an adsorbent. For a more detailed study of the structure of the synthesized NZVI/Zelite, TEM images were prepared (Fig. 3). The images show the uniform distribution of iron nanoparticles on zeolite.

## Response Surface Methodology Modeling and Optimization for Cu(II) Removal

To investigate the effect of operating parameters on Cu(II) removal, a CCD Design based on the experimental design was used. The design of the experiment to study the methodology of the response level was carried out using Design-Expert software (version: 7.0.1) and 30 series of experiments were proposed to study the effect of four effective parameters (Cu<sup>2+</sup> concentration, pH, dosage, and contact time) on the removal of Cu(II). The design of the experiment and its results are given in Table 1. These results were used to implement the RSM model and a quadratic polynomial equation was used to perform regression analysis. The obtained equation between the response (Cu(II)

removal percentage) and each of the independent NZVI/Zeolite factors was expressed from Eq. (2):

$$R = +94.35 + 8.91A + 12.07B - 6.39C + 0.9892D - 8.08AB + 3.90AC - 1.71AD + 5.74BC - 2.78BD + 0.3713CD - 3.03A^2 - 6.63B^2 - 0.9277C^2 + 0.5098D^2 \quad (2)$$

ANOVA (Analysis of Variance) was used to evaluate the statistical significance of each factor and their mutual influence on Cu(II) removal efficiency using Design Expert software. The results of analysis variance (ANOVA) and multiple regression coefficients of Cu(II) removal are given in Table 2. In the evaluation of variance analysis ANOVA, the higher the F value of the model and the lower the

**Table 2.** Analysis of Variance

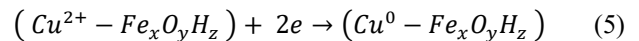
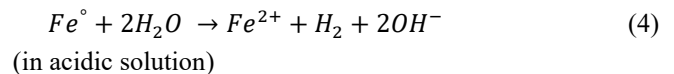
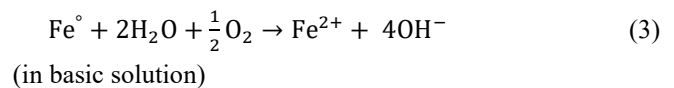
Source	Sum of squares	df	Mean square	F Value	p-Value Prob > F
Model	9802.78	14	700.20	72.72	< 0.0001
A-BZ Conc.	1905.31	1	1905.31	197.89	< 0.0001
B-pH	3494.02	1	3494.02	362.89	< 0.0001
C-dosage	981.25	1	981.25	101.91	< 0.0001
D-Time	23.48	1	23.48	2.44	0.1392
AB	1045.23	1	1045.23	108.56	< 0.0001
AC	242.89	1	242.89	25.23	0.0002
AD	46.58	1	46.58	4.84	0.0439
BC	527.62	1	527.62	54.80	< 0.0001
BD	123.43	1	123.43	12.82	0.0027
CD	2.21	1	2.21	0.2290	0.6391
A <sup>2</sup>	251.65	1	251.65	26.14	0.0001
B <sup>2</sup>	1205.30	1	1205.30	125.18	< 0.0001
C <sup>2</sup>	23.61	1	23.61	2.45	0.1382
D <sup>2</sup>	7.13	1	7.13	0.7404	0.4031
Residual	144.42	15	9.63		
Lack of fit	130.03	10	13.00	4.52	0.0549
Pure error	14.39	5	2.88		
Cor total	9947.20	29			
Std. Dev.	3.10	R-Squared	0.9855		
Mean	86.29	Adj R-Squared	0.9719		
C.V. %	3.60	Pred R-Squared	0.9226		
PRESS	23.08	Adeq Precision	31.9932		

p-value, the more compatible the model will be [21]. The significance of the regression model and F-Values shows the significance and the influence of each independent variable [21]. The values of F (72.72) and p (<0.0001) express the significance of the model and the results show that the model can be well used to explain the percentage of Cu(II) removal as a function of the conditions of selected factors. On the other hand, the value of (LOF) = 4.52 and its non-significance shows that the regression equation can be used to explain the relationship between the response variables and the percentage of Cu(II) removal. According to the p-value, A, B, C, AB, AD, AC, BC, BD, A<sub>2</sub>, B<sub>2</sub>, and C<sub>2</sub> variables are statistically significant, while D, CD, C<sub>2</sub>, and D<sub>2</sub> are not significant (p > 0.05). In addition, the R<sup>2</sup> value of the regression equation was 0.9855, which shows the accuracy of good modeling. Therefore, the regression model can be used to predict the removal of Cu(II) from aqueous solutions.  $R_{Pred}^2$  and  $R_{Adj}^2$  are also very high in this modeling and confirms the suitability of the model with the results of the experiment and it can well predict the desired response. Also, Adeq Precision > 4 indicates the efficiency of the model in the range of design points [22].

To study the validity of the resulting studies, the residual values (the difference between experimental responses and predicted responses) have been calculated. In Fig. 4, the distribution of the residual values is plotted according to the resulting frequency percentage (normal distribution). The linearity of the normal distribution curve for the residuals indicates that the presented model is correct. Also, the residual values in terms of predicted values are shown in Fig. 4. The randomness of the distribution of the residuals indicates the correctness of the selected model. The predictability of the model is finally confirmed by the Box-Cox plot. The Box-Cox plot is a tool to help determine the most appropriate power transfer function to apply to the response. The lowest point in the Box-Cox diagram shows the best  $\lambda$  value in which the minimum residual sum of squares is created in the transformed model. When the ratio of the maximum to the minimum response value is greater than three, there will be more ability to improve the model using the power function. The value of  $\lambda = 1$  indicates the normality of the data. As seen, the value of  $\lambda = 1$ . So, no transformation is needed for the response. The Cook's Distance diagram represents the outlier data and shows the

relationship between the data and the response. If the data is close to one, it means that the data is the outlier and there is a possibility of error in the results. Therefore, the data must be repeated. The Cook's Distance diagram of Cu(II) adsorption is shown that the data are not outliers.

The three-dimensional plots of the surface adsorption of Cu(II) on NZVI/Zeolite are presented in Fig. 5. Figure 5a shows the simultaneous effects of the dosage and the pH of the solution. As shown, both have a positive effect on the Cu(II) removal. The removal process is usually carried out in four ways: adsorption, reduction, precipitation of hydroxide, and electron transfer. Depending on the pH of the solution, Cu ions are found as divalent ion form in pH < 6.5 and as Cu(OH)<sup>+</sup>, Cu(OH)<sup>2+</sup>, and Cu(OH)<sup>3+</sup> in pH = 7.0-9.5 [23]. Generally, for Cu<sup>2+</sup> with E<sup>0</sup> higher (+0.34 V) than E<sup>0</sup> of Fe (0.447 V), the interaction is preferentially through a main redox (iron metal) and precipitation mechanism (Eqs. ((3)-(5)).



The maximum Cu(II) ions removal occurred at pH 8.0-9.5 due to the generation of OH after reduction with Fe<sup>0</sup>. Hence, some Cu(II) ions could be removed by precipitation on the outer layer surface with assistance from some beneficial groups, compounds, and impurities [24]. On the other hand, with the increase of the dosage, the available specific surface area and the active sites are enhanced and therefore the adsorption of Cu(II) is increased [22]. Figure 5b shows the interaction effects of initial Cu(II) concentration and contact time, where a negative effect of initial Cu(II) concentration and a positive effect of contact time are observed. The positive effect of contact time can be attributed to the increased contact time between Cu(II) and NZVI/Zeolite adsorbent [12]. Considering the negative effect of increasing the initial concentration of copper(II) on the removal of copper(II), it can be said that most of the active

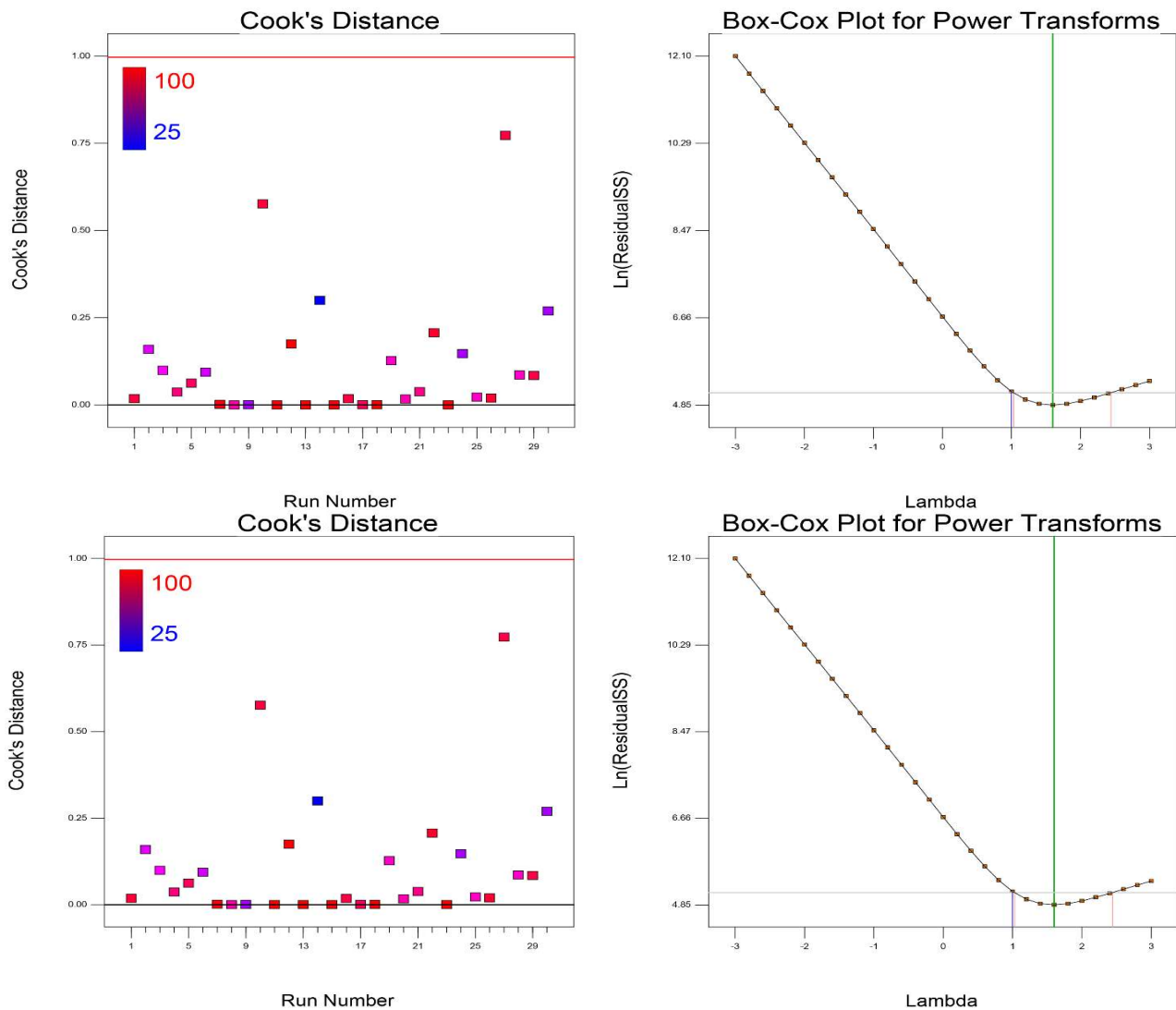


**Fig. 4.** Normal plot of residuals, Curve of predicted and residual values, box-cox diagram, and Cook's Distance diagram of Cu(II) adsorption onto NZVI/Zeolite.

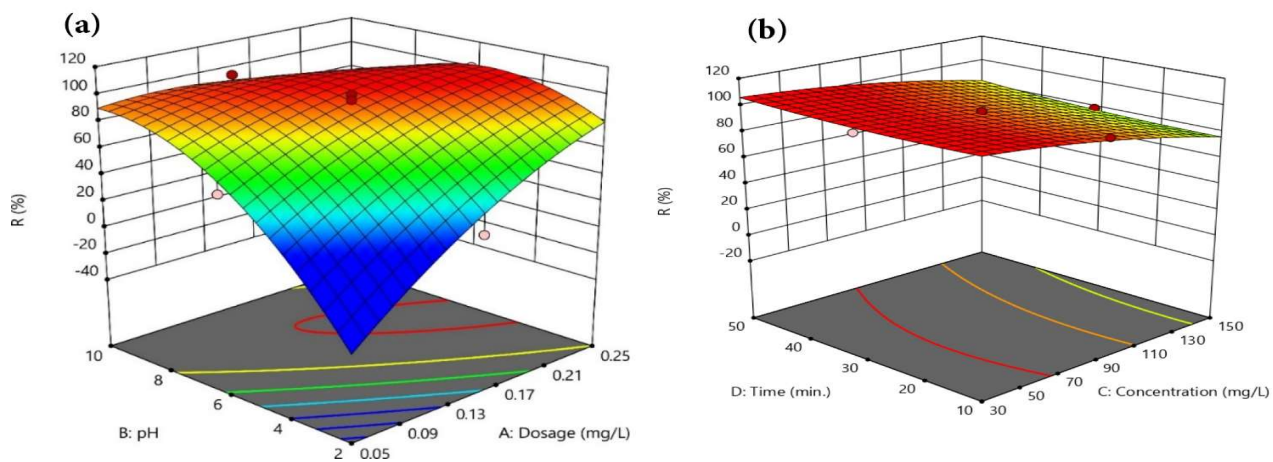


**Fig. 5.** Three-dimensional interaction plots of a) pH and dosage ( $\text{mg l}^{-1}$ ); b) Time (min.) and Concentration ( $\text{mg l}^{-1}$ ).



sites are occupied in the initial concentration, which leads to the deactivation of the NZVI/Zeolite adsorption sites and, as a result, the surface adsorption capacity NZVI/Zeolite reduces [25].

Typically, optimization is the last step in experimental design. In the present study, the suggested optimal conditions by the software are as follows: Dosage = 0.1 g/50 ml; pH = 8,  $[Cu^{2+}]_0 = 60 \text{ mg l}^{-1}$ , Time = 30 min. Experimenting by including the optimal conditions resulted in a destructive efficiency of about 94.77%, which was in good agreement with the theoretical efficiency (95.7%) and confirmed the correctness of the proposed RSM model.

### Adsorption Isotherms

To better understand the adsorption mechanism of the adsorbed ion on the adsorbent, the data were analyzed using isotherm models. Adsorption isotherms are equations that show the distribution of the adsorbed substance between the dissolved and adsorbed phases in the equilibrium at a certain temperature. Among isotherm models, Freundlich, Langmuir, and Temkin isotherms are more widely used [20]. To describe the equilibrium state, two parameters  $q_e$  and  $C_e$  are used, where  $q_e$  is the amount of substance adsorbed per unit weight of the adsorbent and  $C_e$  is the concentration of the Cu(II) remaining in the solution. The results of these three isotherms are shown in Table 3. According to the results (high value of  $R^2$ ), the adsorption of Cu(II) by NZVI/Zeolite follows the Temkin isotherm.

**Reusability of adsorbent.** For this purpose, the possibility of reusing NZVI/Zeolite for up to 5 cycles under optimal conditions based on RSM was evaluated, which is important from a practical point of view. After each use, the NZVI/Zeolite was washed, dried in the oven, and used again.

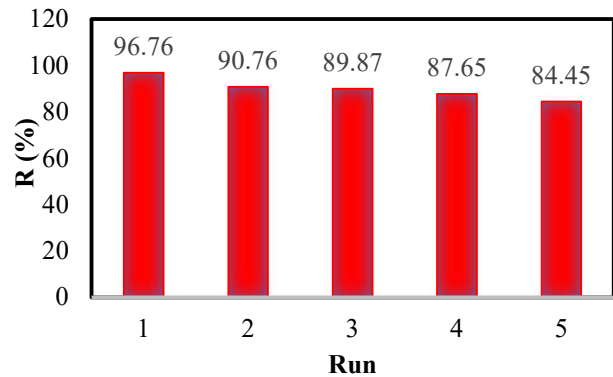


**Fig. 6.** Reusability of NZVI/Zeolite in Cu(II) removal pH = 8, dosage = 0.1 mg l<sup>-1</sup>, Cu(II) concentration = 60 mg l<sup>-1</sup>, and time = 30 min.

As shown in Fig. 6 after 5 times of NZVI/Zeolite use, there was a slight decrease in Cu(II) removal efficiency. The slight decrease in efficiency is probably due to the loss of NZVI/Zeolite during washing, which reduces the removal activity [13]. So, it can be concluded that NZVI/Zeolite can be reused for several periods without significantly reducing its efficiency. This shows the stability and economy of synthesized NZVI/Zeolite.

In Table 4, the efficiency of NZVI/Zeolite in Cu ions removal is compared with zeolite or NZVI-derived adsorbents.

### CONCLUSION

In this study, zero-valent iron nanoparticles based on zeolite were synthesized and applied as an adsorbent for removing Cu(II) from aqueous solutions. XRD, FTIR, FESEM, and TEM were applied to characterize the

**Table 3.** Calculated Isotherms Parameters

Isotherms	Langmuir		Freundlich			Temkin			
Equation	$\frac{1}{q_e} = \left(\frac{1}{K_L q_m}\right) \frac{1}{C_e} + \frac{1}{q_m}$		$\ln q_e = \frac{1}{n} \ln C_e + \ln K_F$			$q_e = B_1 \ln C_e + B_1 \ln K_T$			
Plot	1/q <sub>e</sub> vs. 1/C <sub>e</sub>		ln q <sub>e</sub> vs. ln C <sub>e</sub>			q <sub>e</sub> vs. ln C <sub>e</sub>			
Parameters	R <sup>2</sup>	K <sub>L</sub>	q <sub>m</sub>	R <sup>2</sup>	K <sub>F</sub>	n	R <sup>2</sup>	K <sub>T</sub>	B <sub>1</sub>
Unit	-	l mg <sup>-1</sup>	mg g <sup>-1</sup>	-	mg g <sup>-1</sup>	-	-	L/g	-
Value	0.773	6.75	61.72	0.722	37.64	4.34	0.894	376.15	7.041

**Table 4.** A Comparison of Removal of Cu(II) by NZVI/Zeolite with Another Adsorbent

Adsorbent	Adsorption capacity (mg g <sup>-1</sup> )	Ref.
NZVI	54.35	[23]
mats-supported NZVI	107.8	[24]
NZVI-Kaol	39	[25]
NZVI-kaol	33.74	[26]
ZVI/sand mixture	13.3	[27]
Fly Ash-Derived Zeolite	35.53	[28]
NZVI/Zeolite	61.72	This paper

NZVI/Zeolite. Central Composite Design is carried out as an RSM design. According to the ANOVA, the Cu(II) concentration and pH have a higher effect on Cu(II) adsorption onto NZVI/Zeolite. The results showed that the optimal conditions for Cu(II) removal on NZVI/Zeolite were pH = 8, dosage = 0.1 mg l<sup>-1</sup>, Cu(II) concentration = 60 mg l<sup>-1</sup>, and time = 30 min. Also, the Temkin isotherm model was appropriate for the adsorption of Cu(II) onto NZVI/Zeolite. The results of the experiments showed the high potential capacity of zeolite-based zero-valent iron nanoparticles to remove Cu(II) from aqueous solutions.

## REFERENCES

- [1] Lin, G.; Zeng, B.; Li, J.; Wang, Z.; Wang, S.; Hu, T.; Zhang, L., A systematic review of metal organic frameworks materials for heavy metal removal: synthesis, applications and mechanism. *Chem. Eng. J.*, **2023**, *460*, 141710-141738. <https://doi.org/10.1016/j.cej.2023.141710>.
- [2] Briffa, J.; Sinagra, E.; Blundell, R., Heavy metal pollution in the environment and their toxicological effects on humans. *Heliyon*, **2020**, *6*, e04691-e04716. <https://doi.org/10.1016/j.heliyon.2020.e04691>.
- [3] Joseph, L.; Jun, B. M.; Flora, J. R.; Park, C. M.; Yoon, Y., Removal of heavy metals from water sources in the developing world using low-cost materials: A review. *Chemosphere*, **2019**, *229*, 142-159. <https://doi.org/10.1016/j.chemosphere.2019.04.198>.
- [4] Zeng, B.; Lin, G.; Li, J.; Wang, W.; Zhang, L., Selective removal of mercury ions by functionalized Ti-Zr bimetallic coordination polymers. *Process Saf. Environ. Prot.*, **2022**, *168*, 123-132. <https://doi.org/10.1016/j.psep.2022.09.070>.
- [5] Zhu, J.; Zhang, L.; Liu, J.; Zhong, S.; Gao, P.; Shen, J., Trichloroethylene remediation using zero-valent iron with kaolin clay, activated carbon and bacteria. *Water Res.*, **2022**, *226*, 119186-119197. <https://doi.org/10.1016/j.watres.2022.119186>.
- [6] Hassanzadeh, P.; Gharbani, P.; Derakhshanfard, F.; Memar Maher, B., Preparation and Characterization of PVDF/g-C<sub>3</sub>N<sub>4</sub>/Chitosan Polymeric Membrane for the Removal of Direct Blue 14 Dye. *J. Polym. Environ.*, **2021**, *29*, 3693-3702. <https://doi.org/10.1007/s10924-021-02145-y>.
- [7] Arshadi, M.; Soleymanzadeh, M.; Salvacion, J. W. L.; SalimiVahid, F., Nanoscale zero-valent iron (NZVI) supported on singulas waste for Pb(II) removal from aqueous solution: kinetics, thermodynamic and mechanism. *J. Colloid Interface. Sci.*, **2014**, *426*, 241-51. <https://doi.org/10.1016/j.jcis.2014.04.014>.
- [8] Kong, X.; Han, Z.; Zhang, W.; Song, L.; Li, H., Synthesis of zeolite-supported microscale zero-valent iron for the removal of Cr<sup>6+</sup> and Cd<sup>2+</sup> from aqueous solution. *J. Environ. Manage.*, **2016**, *169*, 84-90. <https://doi.org/10.1016/j.jenvman.2015.12.022>.
- [9] Yu, S.; Liu, J.; Yin, Y.; Shen, M., Interactions between engineered nanoparticles and dissolved organic matter: A review on mechanisms and environmental effects. *J. Environ. Sci.*, **2018**, *63*, 198-217. <https://doi.org/10.1016/j.jes.2017.06.021>.
- [10] Rashtbari, Y.; Américo-Pinheiro, J. H. P.; Bahrami, S.;

- Fazlzadeh, M.; Arfaeina, H.; Poureshgh, Y., Efficiency of zeolite coated with zero-valent iron nanoparticles for removal of humic acid from aqueous solutions. *Water, Air, Soil Pollut.*, **2020**, *231*, 514-524. <https://doi.org/10.1007/s11270-020-04872-9>.
- [11] Arancibia-Miranda, N.; Baltazar, S. E.; García, A.; Muñoz-Lira, D.; Sepúlveda, P.; Rubio, M. A.; Altbir, D., Nanoscale zero valent supported by zeolite and montmorillonite: template effect of the removal of lead ion from an aqueous solution. *J. Hazard. Mater.*, **2016**, *301*, 371-80. <https://doi.org/10.1016/j.jhazmat.2015.09.007>.
- [12] Mehrizad, A.; Gharbani, P., Application of central composite design and artificial neural network in modeling of reactive blue 21 dye removal by photo-ozonation process. *Water Sci. Technol.*, **2016**, *74*, 1115-1126. <https://doi.org/10.2166/wst.2016.199>.
- [13] Fathi, E.; Gharbani, P., Modeling and optimization removal of reactive Orange 16 dye using MgO/g-C<sub>3</sub>N<sub>4</sub>/zeolite nanocomposite in coupling with LED and ultrasound by response surface methodology. *Diam. Relat. Mater.*, **2021**, *115*, 108346. <https://doi.org/10.1016/j.diamond.2021.108346>.
- [14] Li, Z.; Wang, L.; Meng, J.; Liu, X.; Xu, J.; Wang, F.; Brookes, P., Zeolite-supported nanoscale zero-valent iron: New findings on simultaneous adsorption of Cd(II), Pb(II), and As(III) in aqueous solution and soil. *J. Hazard. Mater.*, **2018**, *344*, 1-11.
- [15] Mohseni-Bandpi, A.; Elliott, D. J.; Zazouli, M. A., Biological nitrate removal processes from drinking water supply, *J. Rev. Environ. Health Sci. Eng.*, **2013**, *11*, 35-46.
- [16] He, Y.; Fang, T.; Wang, J.; Liu, X.; Yan, Z.; Lin, H.; Li, F.; Guo, G., Insight into the stabilization mechanism and long-term effect on As, Cd, and Pb in soil using zeolite-supported nanoscale zero-valent iron. *J. Clean. Prod.*, **2022**, *355*, 131634.
- [17] Canafoglia, M. E.; Lick, I. D.; Ponzi, E. N.; Botto, I. L., Natural materials modified with transition metals of the cobalt group: feasibility in catalysis. *J. Argentine. Chem. Soc.*, **2009**, *97*, 58-68.
- [18] Mansouri, N.; Rikhtegar, N.; Panahi, H. A.; Atabi, F.; Shahraki, B. K., Porosity, characterization and structural properties of natural zeolite-clinoptilolite-as a sorbent. *Environ. Prot. Eng.*, **2013**, *39*, 139-52. <https://doi.org/10.1016/10.5277/EPE130111>.
- [19] Yang, L.; Gao, M.; Wei, T.; Nagasaka, T., Synergistic removal of As(V) from aqueous solution by nanoscale zero valent iron loaded with zeolite 5A synthesized from fly ash. *J. Hazard. Mater.*, **2022**, *424*, 127428.
- [20] Li, Q.; Wang, H.; Chen, Z.; He, X.; Liu, Y.; Qiu, M.; Wang, X. Adsorption-reduction strategy of U (VI) on NZVI-supported zeolite composites via batch, visual and XPS techniques. *J. Mol. Liq.*, **2021**, *339*, 116719.
- [21] Mehrizad, A., Adsorption studies of some phenol derivatives onto Ag-cuttlebone nanobiocomposite: modeling of process by response surface methodology. *Res. Chem. Intermed.*, **2017**, *43*, 4295-4310. <https://doi.org/10.1007/s11164-017-2874-y>.
- [22] Fard, B. H.; Khojasteh, R. R.; Gharbani, P., Preparation and Characterization of Visible-Light Sensitive Nano Ag/Ag<sub>3</sub>VO<sub>4</sub>/AgVO<sub>3</sub> Modified by Graphene Oxide for Photodegradation of Reactive Orange 16 Dye. *J. Inorg. Organomet. Polym. Mater.*, **2018**, *28*, 1149-1157. <https://doi.org/10.1007/s10904-018-0798-7>.
- [23] Wang, J.; Liu, G.; Li, T.; Zhou, C.; Qi, C., Zero-valent iron nanoparticles (NZVI) supported by kaolinite for Cu(II) and Ni(II) ion removal by adsorption: kinetics, thermodynamics, and mechanism. *Aust. J. Chem.*, **2015**, *68*, 1305-1315.
- [24] Ayob, A. F.; Ismail, N.; Teng, T. T.; Abdullah, A. Z., Immobilization of Cu<sup>2+</sup> using stabilized nano zero valent iron particles in contaminated aqueous solutions. *Environ. Prot. Eng.*, **2012**, *38*, 119-131.
- [25] Shirzadeh, M.; Sepehr, E.; Rasouli Sadaghiani, M. H.; Ahmadi, F., Effect of pH, initial concentration, background electrolyte, and ionic strength on cadmium adsorption by TiO<sub>2</sub> and  $\gamma$ -Al<sub>2</sub>O<sub>3</sub> nanoparticles. *Pollution*, **2020**, *6*, 223-35. <https://doi.org/10.22059/poll.2019.286644.666>.
- [26] Hamdy, A., Experimental study of the relationship between dissolved iron, turbidity, and removal of Cu(II) ion from aqueous solutions using zero-valent iron nanoparticles. *Arab. J. Sci. Eng.*, **2021**, *46*, 5543-65.
- [27] Xiao, S.; Ma, H.; Shen, M.; Wang, S.; Huang, Q.; Shi, X., Excellent copper(II) removal using zero-valent iron nanoparticle-immobilized hybrid electrospun polymer nanofibrous mats. *Colloids Surf.*, **2011**, *381*, 48-54.

- [28] Üzümlü, C.; Shahwan, T.; Eroglu, A. E.; Hallam, K. R.; Scott, T. B.; Lieberwirth, I., Synthesis and characterization of kaolinite-supported zero-valent iron nanoparticles and their application for the removal of aqueous  $\text{Cu}^{2+}$  and  $\text{Co}^{2+}$  ions. *Appl. Clay Sci.* **2009**, *43*, 172-181.
- [29] Wang, J.; Liu, G. J.; Li, T. F.; Zhou, C. C.; Qi, C. C., Zero-valent iron nanoparticles (NZVI) supported by kaolinite for Cu(II) and Ni(II) ion removal by adsorption: kinetics, thermodynamics, and mechanism, *Aust. J. Chem.* **2015**, *68*, 1305-1315.
- [30] Tarekegn, M. M.; Hiruy, A. M.; Dekebo, A. H., Correction: Nano zero valent iron (nZVI) particles for the removal of heavy metals ( $\text{Cd}^{2+}$ ,  $\text{Cu}^{2+}$  and  $\text{Pb}^{2+}$ ) from aqueous solutions. *RSC Adv.*, **2021**, *11*, 27084.